Anal. Chem. **2002,** *74,* 4536−4547

Anomalous Radial Migration of Single DNA Molecules in Capillary Electrophoresis

Jinjian Zheng and Edward S. Yeung*

Ames Laboratory—USDOE and Department of Chemistry, Iowa State University, Ames, Iowa 50011

We report the unexpected radial migration of DNA molecules in capillary electrophoresis (CE) with applied Poiseuille flow. Such movement can contribute to anomalous migration times, peak dispersion, and size and shape selectivity in CE. When Poiseuille flow is applied from the cathode to the anode, DNA molecules move toward the center of the capillary, forming a narrow, highly concentrated zone. Conversely, when the flow is applied from the anode to the cathode, DNA molecules move toward the walls, leaving a DNA-depleted zone around the axis. We showed that the deformation and orientation of DNA molecules under Poiseuille flow was responsible for the radial migration. By analyzing the forces acting on the deformed and oriented DNA molecules, we derived an expression for the radial lift force, which explained our results very well under different conditions with Poiseuille flow only, electrophoresis only, and the combination of Poiseuille flow and electrophoresis. Factors governing the direction and velocity of radial migration were elucidated. Potential applications of this phenomenon include an alternative to sheath flow in flow cytometry, improving precision and reliability of single-molecule detection, reduction of wall adsorption, and size separation with a mechanism akin to field-flow fractionation. On the negative side, nonuniform electroosmotic flow along the capillary or microfluidic channel is common in CE, and radial migration of certain analytes cannot be neglected.

It is well known that when blood flows through capillaries, the red blood cells tend to migrate toward the center of the capillary, leading to an inhomogeneous distribution of the red blood cells.[1] Jeffery found that particles flowing in a tube have a tendency to concentrate along the flow axis where there are paths of minimal energy dissipation due to the lack of shear forces.[2] Segre and Silberberg found that neutrally buoyant spheres in Poiseuille flow through a tube slowly migrate radially to a position of ∼0.6 tube radii.[3−5] They proposed the existence of an inertial force that is centrifugal and a wall effect that is centripetal. Goldsmith and Mason found that deformable particles tend to rest on the tube axis at very low Reynolds numbers while rigid spheres do not.[6,7] Later, Haber and Hestroni,[8] Whol and Rubinow,[9] and Chan and Leal[10,11] studied the motion of deformable spheres in viscous shear flow theoretically and found a transverse force besides the inertial effect by resolving the creeping flow equation. So far, the practical utility of such effects is not obvious. For example, the axial migration is usually too slow to meet the requirements of flow cytometry, in which particles must be focused into a well-defined path in a short time and within a short distance. Also, the difficulty in controlling the direction and velocity of axial migration limits the application to field-flow fractionation, a separation technique based on the radial distribution of particles in a shear flow.[12]

The radial migration velocity is usually dependent on the particle size. For small particles, the migration velocity is small. Besides, Brownian motion can no longer be neglected. It is therefore interesting to see whether such radial migration applies to single molecules during electrophoresis, with or without shear flow. DNA molecules usually exist as a random coil in aqueous solution. The diameter is on the order of nanometers to micrometers, depending on the number of base pairs. This is much smaller than the particles used in the studies cited above. In capillary electrophoresis without shear flow, the shear stress is negligible and so is the radial migration. Therefore, by comparing the axial positions of single DNA molecules as a function of time during capillary electrophoresis as imaged by an intensified CCD camera, the DNA mobility can be calculated and can be used for high-throughput characterization of DNA molecules.[13,14]

However, we found that, by applying hydrodynamic flow (Poiseuille flow) during capillary electrophoresis, λ-DNA molecules migrate radially in addition to axially, either inward to the capillary axis or outward to the capillary wall. This distorts the assumed homogeneous radial distribution of λ-DNA molecules, producing a high concentration zone either around the axis or near the wall. The radial migration reaches equilibrium in ∼20 s, within an axial migration distance of millimeters. The DNA molecules migrate radially faster despite being smaller compared with the particles in previous studies. Radial migration has implications for separation efficiencies in capillary electrophoresis.

* Corresponding author: (phone) 515-294-8062; (e-mail) yeung@ameslab.gov.

(1) Uijttewaal, W. S.; Nijhof, E. J.; Heethaar, R. M. *J. Biomech.* **1994**, *27*, 35−42.
(2) Jeffrey, G. B. *Proc. R. Soc. London, Ser. A* **1922**, *102*, 161−179.
(3) Segre, G.; Silberberg, A. *Nature* **1961**, *189*, 209−210.
(4) Segre, G.; Silberberg, A. *J. Fluid Mech.* **1962**, *14*, 115−135.
(5) Segre, G.; Silberberg, A. *J. Fluid Mech.* **1962**, *14*, 136−157.
(6) Goldsmith, H. L.; Mason, S. G. *Nature* **1961**, *190*, 1095−1096.
(7) Goldsmith, H. L.; Mason, S. G. *J. Colloid Sci.* **1962**, *17*, 448−476.
(8) Haber, S.; Hestroni, G. *J. Fluid Mech.* **1971**, *49*, 257−277.
(9) Whol, P. R.; Rubinow, S. I. *J. Fluid Mech.* **1971**, *62*, 185−207.
(10) Chan, P. C.-H.; Leal, L. G. *J. Fluid Mech.* **1979**, *92*, 131−170.
(11) Leal, L. G. *Annu. Rev. Fluid Mech.* **1980**, *12*, 435−476.
(12) Giddings, J. C. *Science* **1993**, *260*, 1456−1465.
(13) Shortreed, M. R.; Li, H.; Huang, W.-H.; Yeung, E. S. *Anal. Chem.* **2000**, *72*, 2879−2885.
(14) Ma, Y.; Shortreed, M. R.; Yeung, E. S. *Anal. Chem.* **2000**, *72*, 4640−4645.

10.1021/ac0257344 CCC: $22.00
Published on Web 07/30/2002

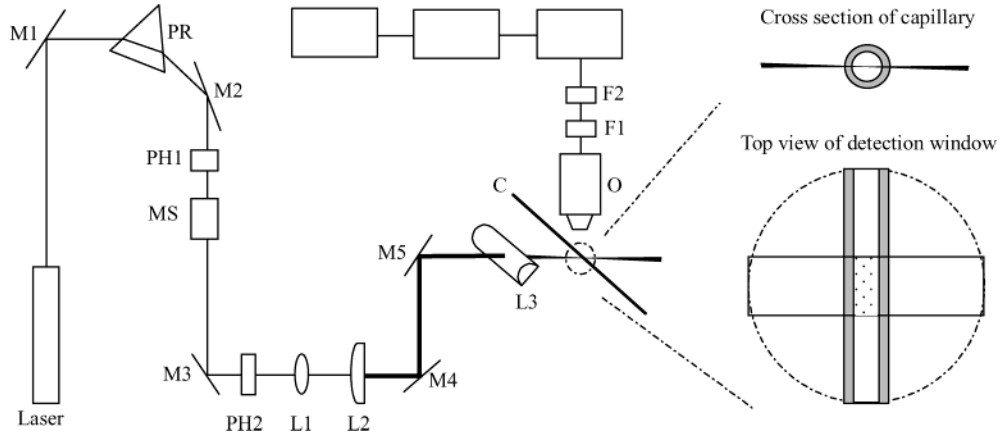

Figure 1. Schematic illustration of the experimental setup: laser, 488-nm cw argon ion laser; MS, mechanical shutter; PR, equilateral prism to remove plasma lines; M1−5, mirrors; PH1−2, pinholes; L1, convex lens, FL = 25 mm; L2, convex lens, FL = 75 mm; L3, cylindrical lens, FL = 15 mm; C, capillary. The expanded inset shows the excitation and detection region: O, objective lens, 10× NA 0.25 for round capillary and 20× NA 0.75 for square capillary; F1 and F2, 488-nm holographic notch filters; ICCD, intensified CCD camera; PG-200, function generator for controlling the ICCD; PC, personal computer for data acquisition and analysis.

At such a time and distance scale, this phenomenon is also relevant to other fields such as flow cytometry, field-flow fractionation, etc. In this work, efforts were directed to study the mechanism of radial migration and the factors governing the migration direction and velocity.

EXPERIMENTAL SECTION

Capillary. We used bare fused-silica, square capillaries (Polymicro, Phoenix, AZ, 75-μm i.d., 365-μm o.d.) or poly(vinyl alcohol) (PVA)-coated round capillaries (Agilent Technology, Palo Alto, CA, 75-μm i.d., 365-μm o.d.) in this study. The bare capillary was flushed with 0.5 mL of 1 mM NaOH solution followed by 1 mL of buffer. A clear window (1 cm long) was created by removing the polymer cladding on the capillary with a window maker (Microsolv, Long Branch, NJ). The window was then cleaned repeatedly with methanol-soaked lens cleaning paper before use. The PVA-coated capillary was flushed with 1 mL of buffer only. Before using the PVA-coated capillary for CE, its electroosmotic flow (EOF) velocity was measured using the following procedure: (1) put 20 mL of 10 mM pH 7.0 Gly-Gly buffer in two 25-mL bottles; (2) equilibrate the liquid level of these two bottles by connecting them with a 1-mm-i.d. Teflon tube filled with same buffer for at least 1 h; (3) fill a 200 mm long, PVA-coated capillary with 2 mM pH 7.0 Gly-Gly buffer and put the ends into the two buffer bottles; (4) remove the Teflon tube; (5) apply an electric field of 62.5 V/cm while monitoring the change in current over time. No change in current was found after applying the electric field for 30 min, indicating that the EOF velocity is extremely low.

To create an optical window, the PVA-coated capillary was filled with deionized water first. The polymer cladding was then removed with concentrated sulfuric acid preheated to near boiling. All capillaries were glued to sturdy Al blocks so that no realignment was necessary between runs. To rinse the capillary or to inject samples into the capillary, a capillary adapter (InnovaQuartz, Inc., Phoenix, AZ) was used to couple the capillary to a syringe. Two 1.5-mL centrifuge tubes were used as buffer reservoirs. One buffer reservoir was fixed to a *Z*-translational microstage to balance the liquid levels of both buffer reservoirs or to apply a desired hydrodynamic flow.

Buffer. The buffers used in this study are designated by the ionic strength. The 5 mM pH 8.0 Gly-Gly (Sigma, St. Louis, MO) buffer was prepared by titrating 5 mM NaOH (Sigma) to pH 8.0 with 50 mM Gly-Gly solution. The buffer was then filtered with a 0.22-μm filter and left for photobleaching overnight with a mercury lamp. The NaCl (Sigma) solution with a concentration of 0.1 M was prepared by dissolving 0.585 g of NaCl in 100 mL of deionized water. This solution was also filtered with a 0.22-μm filter and photobleached overnight with a mercury lamp. Lower concentration NaCl solutions were prepared by diluting the 0.1 M NaCl solution with filtered and photobleached deionized water.

DNA Samples. λ-DNA (48 502 bp, Life Science, Grand Island, NY) and 1 kb ladder DNA samples (Life Science) were labeled with YOYO-1 (Molecular Probes, Eugene, OR) at a ratio of 1 dye molecule/5 bp according to the manufacturer's instructions. Typically, YOYO-1 labeled DNA samples were first prepared as a 200 pM stock solution, incubated at room temperature for at least 1 h, and diluted with corresponding buffer to the desired concentration just prior to the start of the experiment. The concentration of λ-DNA used for the experiments is 0.1 pM unless specified. Since the purpose of this work is to observe the motion of DNA molecules during electrophoresis, the whole capillary was filled with DNA samples instead of a short injected plug.

Experimental Setup. The experimental setup for this study is shown in Figure 1. A Pentamax 512-EFT/1EIA intensified-CCD camera (ICCD, Princeton Instruments, Princeton, NJ) was mounted on top of a Zeiss Axioskop upright microscope. The programmable function generator was also from Princeton (PG-200). The digitization rate of the camera was 5 MHz (12 bits) with the software controller gain set at 3 and the hardware intensifier gain set at 750 V. The camera was operated in the external synchronization mode with the intensifier disabled-open and was also used in the frame-transfer mode.

A 488-nm argon ion laser (Uniphase, San Jose, CA) was used as the excitation beam. Unless specified, the laser power was set at 5 mW. As shown in Figure 1, the laser beam was refracted by an equilateral dispersing prism and transmitted through an optical pinhole to eliminate extraneous light and plasma lines from the

laser. A Uniblitz mechanical shutter (model LS2Z2, Vincent Associates, Rochester, NY) was used to block the laser beam when the camera was off to reduce photobleaching. The shutter was controlled by a model T132 shutter driver (Vincent Associates). The ICCD camera was synchronized by connecting the "Sync Output" in the shutter driver to the "Ext Sync" in the ICCD. The "Logic Out" in the ICCD was connected to the "Shutter In" in the PG-200 to shut off the intensifier during the read-out cycle of the ICCD. The sampling frequency was 10 Hz, with the shutter driver set to 10-ms exposure and 90-ms delay unless specified. After the mechanical shutter, the laser beam was refined with a pinhole again and then expanded by two well-positioned convex lenses, which served as a beam expander. The expanded beam was then focused into the capillary at normal angle as a thin sheet with a cylindrical lens (focal length, 15 mm; Edmund Industrial Optics, Barrington, NJ). The image of the laser focusing plane was schematically shown in the enlarged part in Figure 1. With this excitation mode, only molecules inside the laser focusing plane ($\sim$10 μm thick) could be excited and detected. It is worth noting that the mirror M5, the cylindrical lens, and the capillary were fixed to the stage of the microscope so that the focus would not change when the capillary was moved up and down under the microscope. Fluorescence from single molecules was collected by a Zeiss 20×/0.75 NA Plan-Apochromat microscope objective lens. Two 488-nm holographic notch filters (Kaiser Optical, Ann Arbor, MI; HNFP) with optical density of >6 were placed between the objective lens and the ICCD to cut off the scattering from the excitation beam. Data acquisition was through the WinView software provided by Princeton Instruments.

Data Analysis Algorithm. The WinView data file recorded the fluorescence images of DNA molecules within the field of view, which was about 75 μm wide and 400 μm long. From this "movie", we can directly obtain quantitative information on the migration behavior of DNA molecules, such as moving toward the axis or the walls. With an in-house computer program, the number of DNA molecules with respect to their radial positions and time can be obtained. Since only molecules in the center plane were excited and counted, the migration of DNA molecules toward the axis would result in an increase in the observed molecule number, until equilibrium was reached. On the other hand, the observed DNA molecule number decreased if DNA molecules moved toward the walls, until equilibrium was reached. Therefore, by plotting the DNA molecule number against time, we were able to calculate the time for the DNA molecules to reach positional equilibrium. In addition, the average molecule numbers at specific radial positions can be calculated, providing precise information on the radial distribution of DNA molecules at different periods. Due to the symmetry of the capillary, the two-dimensional results obtained here can be easily extended to the planes above and below the laser focus to provide a three-dimensional picture.

RESULTS

1. Motion of DNA Molecules in a Capillary under Hydrodynamic Flow. Images of DNA molecules driven by hydrodynamic flow through a 200-cm-long, 75-μm-i.d. bare fused-silica, square capillary were recorded. Flow velocity at the axis was 1 mm/s as measured from the single-molecule movies. The DNA molecules flowed through the observed region without changing their radial position. Figure 2a is the average DNA molecule number at each radial position through 1000 frames (or 200 s). The relative radial position 0.5 refers to the center of the capillary, while 0 and 1 are walls. In Figure 2a, there was a slight bias to higher molecule numbers on the left side that was due to the higher laser intensity (more efficient excitation) at the focal point. Otherwise, DNA molecules were homogeneously distributed within the capillary. Figure 2b shows the total molecule number in each frame. The total molecule number did not change with time, indicating that there was no change in the radial molecule distribution.

Usually, the flow inside a channel is characterized with a dimensionless quantity named the Reynolds number.[15,16] The Reynolds number in Figure 2 was 0.075, indicating that the flow was laminar. This is consistent with the lack of radial bias in the molecule numbers. Maintaining the same conditions as in Figure 2, we repeated this experiment for periods up to 30 min using higher hydrodynamic flow velocities of 2, 5, 10, and 20 mm/s. The corresponding Reynolds numbers were 0.15, 0.375, 0.75, and 1.5. Similar to the results in Figure 2, no obvious radial migration was observed.

2. Motion of DNA Molecules in Capillary Electrophoresis without Hydrodynamic Flow. A dc power supply was used to apply an electric field of −40 V/cm through the same fused-silica, square capillary as in Figure 2 for electrophoresis. The electrophoretic migration was from cathode (−) to anode (+), but the motion of DNA molecules was from anode (+) to cathode (−) because the electroosmotic mobility was higher than the electrophoretic mobility in the bare capillary. As shown in Figure 3a, similar radial distribution of DNA molecules was observed compared to Figure 2a. This is also consistent with the measurements of the trajectories of individual DNA molecules.[13] Figure 3b shows that the total molecule number did not change with time, confirming that there was no change in molecule distribution during capillary electrophoresis, as predicted by the expected flat flow profile.[17]

3. Motion of DNA Molecules in Capillary Electrophoresis with Hydrodynamic Flow. The capillary electrophoresis conditions were the same as those in Figure 3. However, before applying the electric field, a hydrodynamic flow from cathode to anode was created by lifting the cathodic buffer reservoir. The cathodic buffer reservoir was lifted by 23.5 mm with a *z*-axis stage, which produced a hydrodynamic flow of $\sim$340 μm/s at the axis of the capillary. Figure 4a is the sequence of four images of DNA molecules inside the 75-μm-i.d. bare fused-silica, square capillary after applying an electric field of −40 V/cm for 0, 10, 20, and 30 s. With time, the initially homogeneously distributed DNA molecules began to move toward the axis. The radial distribution of DNA molecules before and after electrophoresis is shown in Figure 4b. Since the concentration of DNA sample is only 0.1 pM, the molecule distribution in the first frame of Figure 4a does not need to be homogeneous. However, the average results of 100 frames in Figure 4b show that DNA molecules are homogeneously

(15) Nevers, N. *Fluid Mechanics for Chemical Engineers*, 2nd ed.; McGraw-Hill: New York, 1991; Chapter 6.
(16) Van Dillar, M. A.; Dean, P. N.; Laerum, O. D.; Melamed, M. R. *Flow Cytometry: Instrumentation and Data Analysis*; Academic Press: New York, 1985; Chapter 3.
(17) Rice, C. L.; Whitehead, R. *J. Phys. Chem.* **1965**, *69*, 4017−4024.

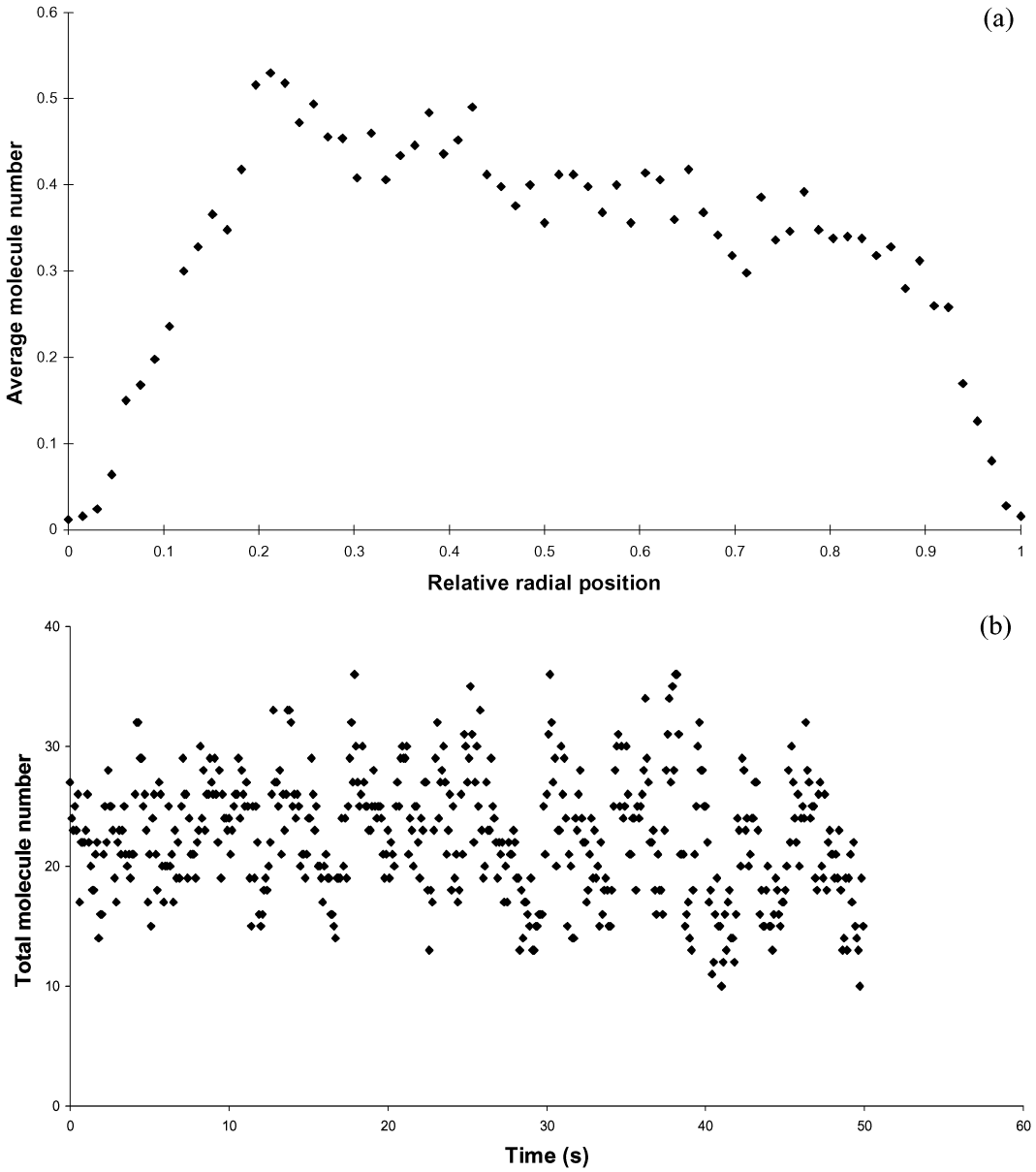

Figure 2. Motion of λ-DNA molecules in a capillary with applied Poiseuille flow. (a) Statistical results of 1000 frames showing the radial distribution of DNA molecules, presented as the average molecule number at each radial position; (b) change in the total molecule number in each frame after applying Poiseuille flow: sample, 0.1 pM λ-DNA in 5 mM Gly-Gly buffer (pH 8.0); capillary, 200-cm-long, 75-μm-i.d. bare fused-silica, square capillary; flow velocity, 1 mm/s; shutter, 5-ms exposure time and 195-ms delay time; laser, 10 mW.

distributed within the capillary before applying an electric field. On applying the electric field, DNA molecules were focused to a 15-μm zone around the axis. There were no molecules near the walls. By plotting the total molecule number in each frame against time, as shown in Figure 4c, we were able to determine the equilibration time, which was ~18 s in this experiment.

When hydrodynamic flow was applied from anode to cathode, the sequence of four images of DNA molecules obtained after applying an electric field of −40 V/cm for 0, 10, 20, and 30 s is shown in Figure 5a. The results were opposite to those in Figure 4a. After applying the electric field, DNA molecules migrate toward the walls, so that finally there were no DNA molecules in the center zone, as shown in Figure 5b. The change of total molecule number with time is plotted in Figure 5c. In Figure 5c, the direction of hydrodynamic flow was changed repeatedly. The symbol "+" refers to hydrodynamic flow from cathode to anode, and "−" refers to hydrodynamic flow from anode to cathode. It is clear that DNA molecules migrated toward the wall or to the axis almost as soon as the hydrodynamic flow direction was changed.

Comparing Figures 4b and 5b, we can find that the concentration of DNA molecules at the center region increased by ~20 times after inward migration while that near the wall increased only ~1.5 times after outward migration. However, this does not mean that the radial force toward the center of the capillary is stronger than that toward the edge. The number of DNA molecules in a given length of capillary should be constant with or without radial migration. The results in Figures 4c and 5c are related to our detection mode as shown in Figure 1. Since only molecules at the 10-μm-thick excitation plane can be detected, an inward radial migration causes more molecules to move into the excitation plane, while an outward radial migration forces molecules to move out of the excitation plane.

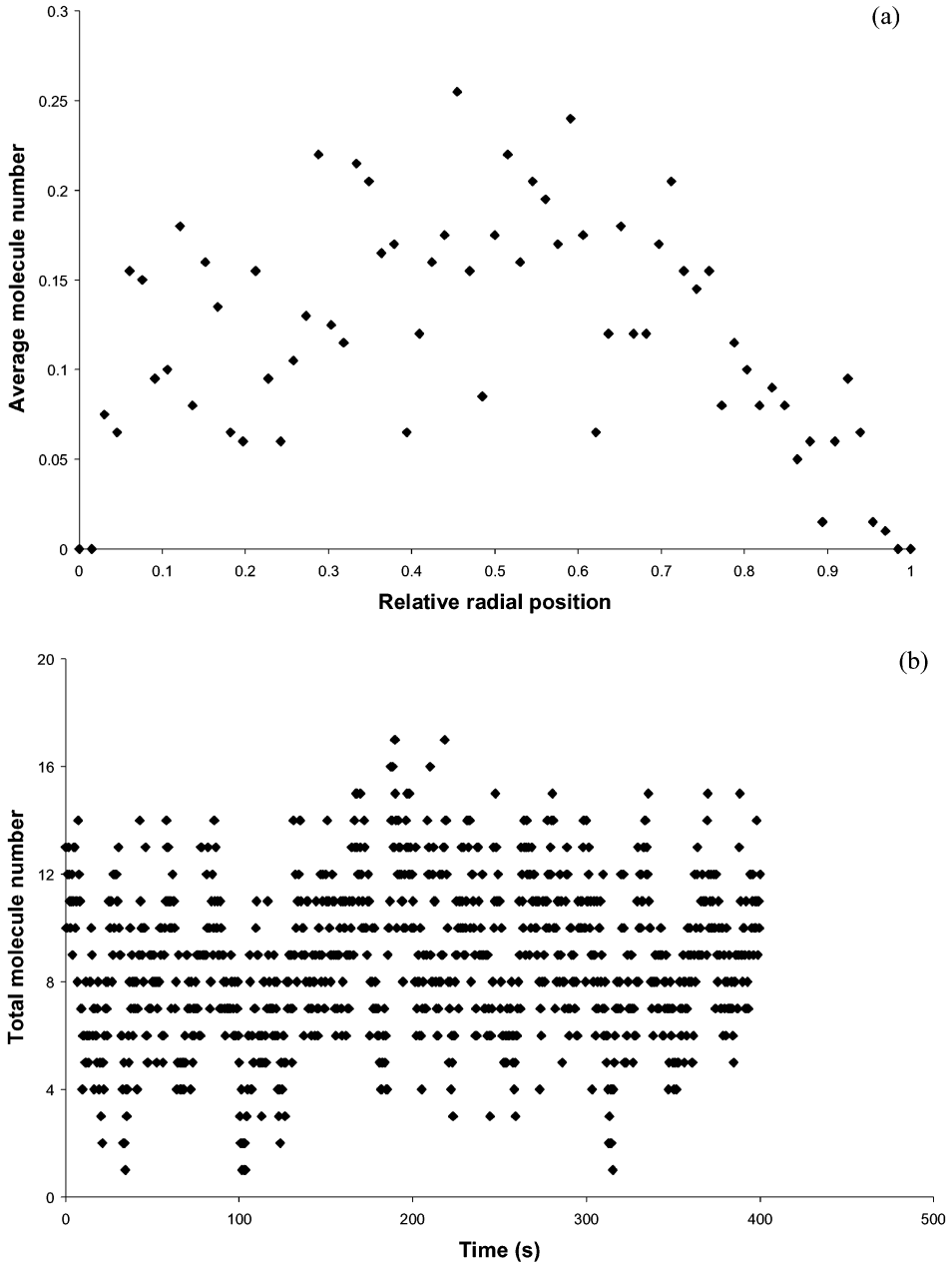

Figure 3. Motion of λ-DNA molecules in capillary electrophoresis without Poiseuille flow. (a) Statistical results of 1000 frames showing the radial distribution of DNA molecules, presented as the average molecule number at each radial position; (b) change in the total molecule number in each frame after applying electric field: sample, 0.1 pM λ-DNA in 5 mM Gly-Gly buffer (pH 8.0); capillary, 31-cm-long, 75-μm-i.d. bare fused-silica, square capillary; electric field, −40 V/cm; shutter, 10-ms exposure time and 390-ms delay time; laser, 5 mW.

DISCUSSION

Radial migration of DNA molecules implies a force perpendicular to the flow and the electric field that drives DNA molecules to migrate axially. There are two possible radial forces: electrostatic force from the charged capillary wall and (or) hydrodynamic force due to the shear gradient of Poiseuille flow.

Electrostatic force may play an important role when the ionic strength of the buffer is very low and DNA molecules are near the wall. For example, experiments similar to that in Figure 3 were performed except that the buffer (5 mM pH 8.0 Gly-Gly buffer) was replaced with 5 μM NaCl. Radial migration of DNA away from the wall of the capillary was found after applying an electric field. However, this occurred only in the region <4 μm away from the wall. When a buffer with 5 mM ionic strength was used, the electric double layer was much thinner compared to the capillary diameter so that the electrostatic force could be neglected. Besides, electrostatic force can only point inward but not outward. Therefore, it cannot cause the results in Figure 5, in which DNA molecules migrate toward the wall. To further explore the effects of electrostatic force, we performed the same experiment as in Figure 4 except that a PVA-coated capillary was used instead of the bare, fused-silica capillary. The results are shown in Figure 6. Radial migration of DNA was also observed, either inward or outward, in a similar manner as the bare capillary. As described in the Experimental Section, the EOF of the PVA-coated capillary was nearly zero, indicating that the surface charge density was negligible. Therefore, we can conclude that electro-

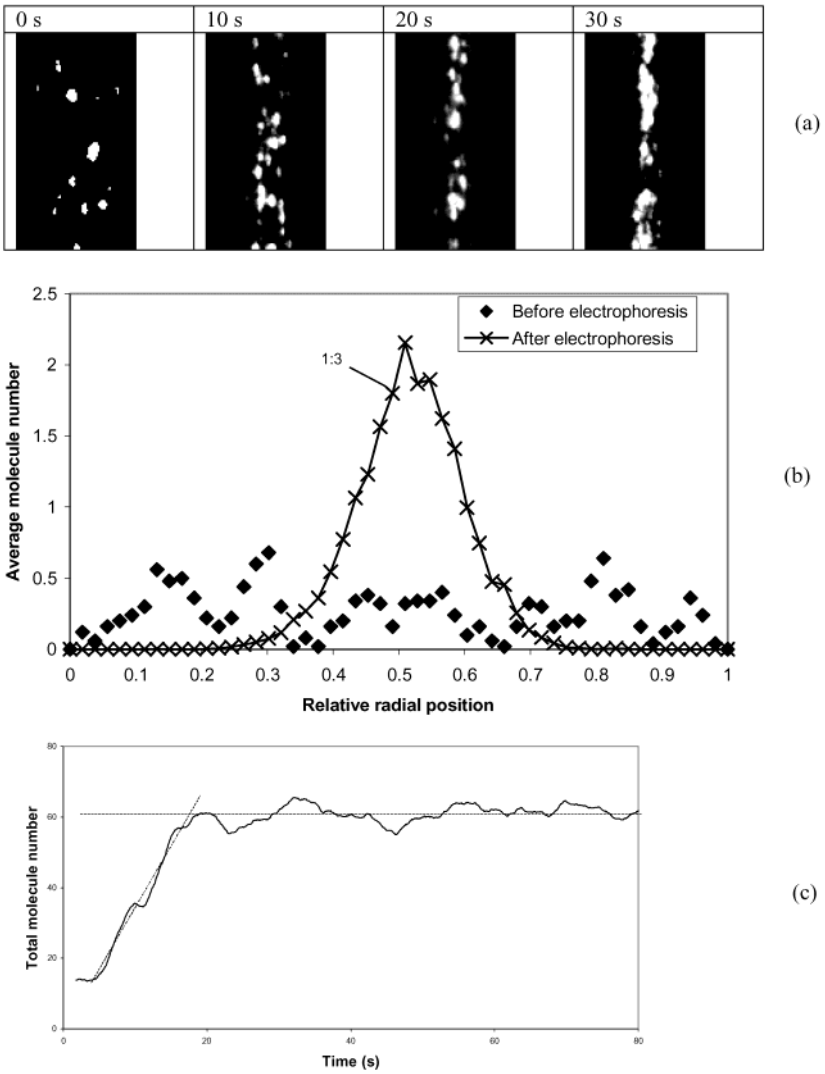

Figure 4. Motion of λ-DNA molecules in capillary electrophoresis with Poiseuille flow from cathode to anode. (a) Images showing inward migration of DNA molecules after applying an electric field for 0, 10, 20, and 30 s; (b) comparison of the radial distribution of DNA molecules before (◆) and after ($\times$ and solid line) applying electric field; and (c) change in the total molecule number in each frame after applying electric field: sample, 0.1 pM λ-DNA in 5 mM Gly-Gly buffer (pH 8.0); capillary, 31-cm-long, 75-μm-i.d. bare fused-silica, square capillary; electric field, −40 V/cm; hydrodynamic flow, from cathode to anode with a maximum velocity of 340 μm/s; shutter, 10-ms exposure time and 90-ms delay time; laser, 10 mW.

static force was not the primary cause of radial migration in these studies.

For Poiseuille flow through a round tube, the velocity profile, v, at a position r from the axis can be expressed as[15]

$$v = v_0(1 - r^2/r_0^2) \quad (1)$$

in which r_0 is the tube radius. The flow has a maximum velocity v_0 at the axis and is 0 at the walls.

When a particle is placed in a shear flow such as Poiseuille flow, the flow velocity is different on the two sides. This produces a torque that is proportional to the shear gradient rate G. The shear gradient rate G can be obtained by differentiating eq 1.

$$G = \mathrm{d}v/\mathrm{d}r = -(2v_0/r_0^2)r \quad (2)$$

Rigid spheres will rotate uniformly about an axis orthogonal to the shear field under this torque, while rigid ellipsoidal particles will rotate periodically, with their long axis spending most of the time oriented parallel to the flow.[16] For deformable particles such as cells,[18] liquid drops,[19] and bubbles,[20] the situation is more complicated. These will be deformed and orient along the flow. The degree of deformation and the orientation angle greatly depend on the local shear gradient rate G. Goldsmith found that human red cells at a very low shear rate bent and folded over while rotating.[18] At a high shear rate, the cells were deformed with their major axes oriented at a small angle to the flow. Instead of rotation, the cell contours changed continuously during flow. This was attributed to the internal circulation of the cell contents by analogy to a liquid drop.

The double-stranded DNA molecules used in this experiment are long polymer chains that exist as random coils in aqueous solution due to the hydrophobic forces between nucleosides. If

(18) Goldsmith, H. L. *Biorheology* **1971**, *7*, 235−242.
(19) Zapryanov, A.; Tabakova, S. *Dynamics of Bubbles, Drops and Rigid Particles*; Kluwer Academic Publishers: New York, 1999; Chapters 6 and 8.
(20) Legendre, D.; Magnaudet, J. *J. Fluid Mech.* **1998**, *368*, 81−126.

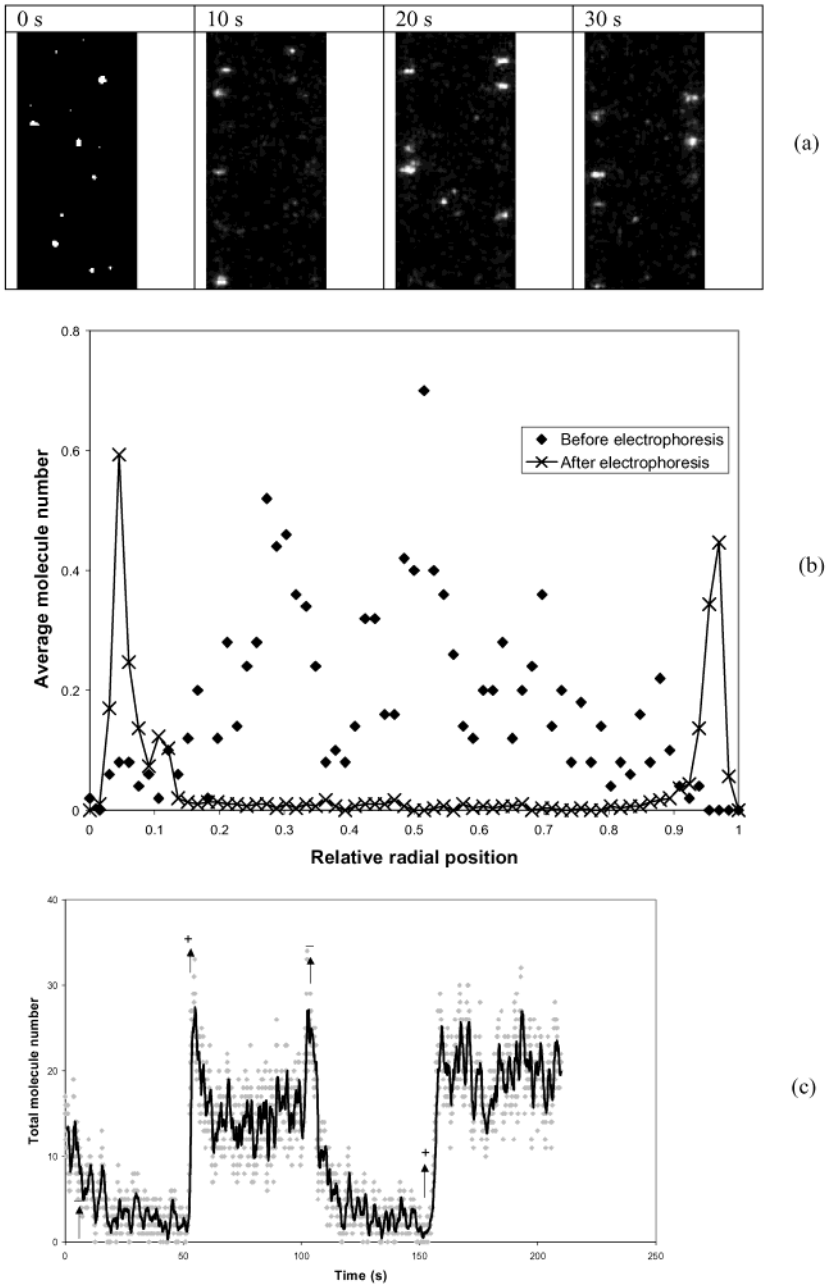

Figure 5. Motion of λ-DNA molecules in capillary electrophoresis with Poiseuille flow from anode to cathode. (a) Images showing outward migration of DNA molecules after applying an electric field for 0, 10, 20, and 30 s; (b) comparison of the radial distribution of DNA molecules before (◆) and after ($\times$ and solid line) applying electric field; and (c) change in the total molecule number in each frame with the change in the relative direction of Poiseuille flow, where ◆ is the raw data and the solid line is the smoothed data: sample, 0.1 pM λ-DNA in 5 μM NaCl; capillary, 31-cm-long, 75-μm-i.d. bare fused-silica, square capillary; electric field, −40 V/cm; hydrodynamic flow, maximum velocity of 340 μm/s; shutter, 10-ms exposure time and 90-ms delay time; laser, 10 mW. The electric field was applied throughout in Figure 5c, but the flow direction was changed repeatedly during the experiment. Flow direction, 0−52 s, anode to cathode; 52−100 s, cathode to anode; 100−153 s, anode to cathode; and 153−210 s, cathode to anode.

the hydrophobic forces between nucleosides are strong enough to overcome shear stress, the coil structure will be maintained. The DNA molecules will then rotate under shear flow. According to the theoretical study of Saffman,[21] Rubinow and Keller,[22] and McLaughlin,[23−25] radial migration toward the axis is predicted when there is hydrodynamic flow. These predictions are consistent with our observations in Figure 4 but are exactly opposite to our observations in Figure 2 and Figure 5. Apparently, the theoretical models of radial migration of rigid spheres do not apply to DNA molecules under the conditions used in this work.

The deformation of large DNA molecules has been reported by several groups. Chu and his group reported the deformation of large DNA molecules under shear flow.[26−28] Shrewsbury et al.

(21) Saffman, P. G. *J. Fluid Mech.* **1965**, *22*, 385−400.
(22) Rubinow, S. I.; Keller, J. B. *J. Fluid Mech.* **1961**, *11*, 447−459.
(23) McLaughlin, J. B. *J. Fluid Mech.* **1991**, *224*, 261−274.
(24) McLaughlin, J. B. *J. Fluid Mech.* **1993**, *246*, 249−265.
(25) Cherukat, P.; McLaughlin, J. B.; Graham, A. L. *Int. J. Multiphase Flow* **1994**, *20*, 339−353.
(26) Perkins, T.; Smith, D. E.; Chu, S. *Science* **1997**, *276*, 2016−2021.

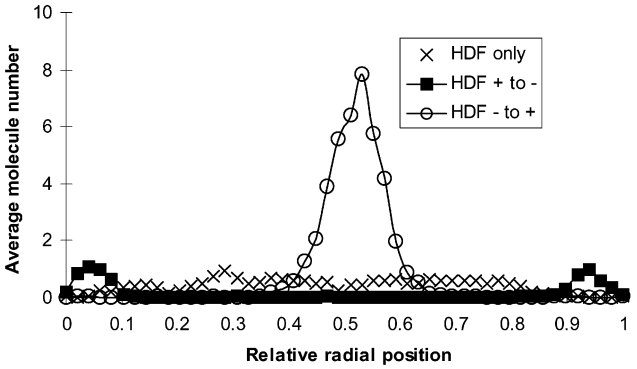

Figure 6. Motion of λ-DNA molecules in PVA-coated capillary. $\times$: radial distribution of λ-DNA molecules in Poiseuille flow without electric field. The average molecule number in each radial position is calculated from 100 frames. Circle and solid line: radial distribution of λ-DNA molecules under electrophoresis with Poiseuille flow applied from cathode to anode. Maximum flow velocity, 115 μm/s. The average molecule number in each radial position is calculated from 300 frames after the radial migration reached equilibrium. Square and solid line, radial distribution of λ-DNA molecules under electrophoresis with Poiseuille flow applied from anode to cathode. Maximum flow velocity, 115 μm/s. The average molecule number in each radial position is calculated from 300 frames after the radial migration reached equilibrium: Sample, 0.1 pM λ-DNA in 5 μM NaCl; capillary, 20-cm-long, 365-μm-o.d., 75-μm-i.d. PVA-coated capillary; electric field, −62.5 V/cm. The EOF velocity in the PVA-coated capillary was undetectable.

observed deformation of λ-DNA in shear flow through microfabricated channels.[29] Li and Larson studied the deformation of DNA and polystyrene, both experimentally and theoretically.[30] Odegaard-Jensen et al. performed computer simulation of DNA orientation and deformation in shear flow.[31] We have documented continuous shape changes and tumbling of single DNA molecules even under slow hydrodynamic flow.[32] On the basis of these results, it is reasonable to treat DNA molecules as deformable particles and not as rigid particles. Figure 7 depicts the deformation and orientation of DNA molecules under shear flow. Due to the difference in flow velocities on the two sides, DNA molecules will be deformed and tilt toward the capillary axis, where there exists the maximum flow velocity. The angle θ is the direction of electrophoretic motion of the DNA molecule with respect to the reference axis of the deformed DNA molecule.

Although there is no report on the radial migration of DNA molecules in shear flow so far, the radial migration of deformable particles such as fiber threads, red blood cells, and liquid drops has been documented since the 1960s in both experimental and theoretical studies.[7−11,19,33] The density of DNA molecules is close to that of the buffer solution. Therefore, they could be considered as neutrally buoyant deformable particles. Although the model of Whol and Rubinow[9] predicted inward radial migration for Poiseuille flow in the absence of an electric field, it was not observed in this work (Figure 2). This could be attributed to the small size of the DNA molecules compared to the capillary inner dimension. However, on applying an electric field, DNA molecules translate relative to the flow in analogy to nonneutrally buoyant particles that are driven by gravity with or against the shear flow. According to Whol and Rubinow,[9] DNA molecules should migrate toward the axis when the flow is from cathode to anode and vice versa. This is similar to our results as shown in Figures 4 and 5. However, due to the complexity of the system, quantitative predictions are difficult. For example, Whol and Rubinow[9] found that Haber and Hestroni's[8] results contained algebraic errors, thus predicting opposite results. Chan and Leal[10,11] reinvestigated this problem, and their results were comparable to those of Whol and Rubinow qualitatively, but the lateral migration velocity was found to be only ~1/10 of that reported by Whol and Rubinow. Besides, DNA molecules are different from liquid drops with respect to surface properties and restoration forces (hydrophobic forces). Therefore, we do not expect to be able to interpret our results quantitatively.

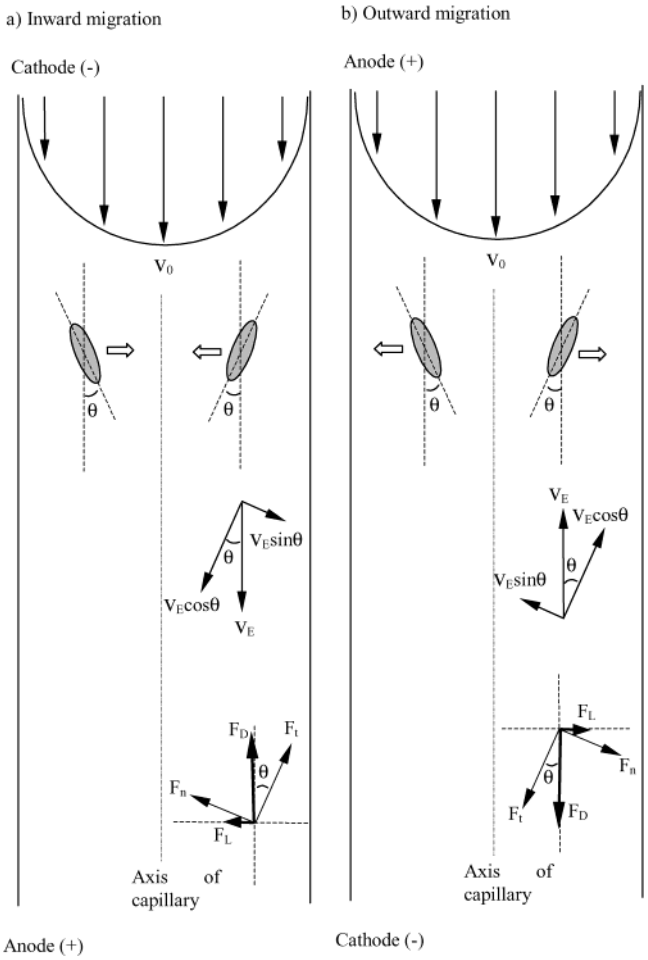

Figure 7. Deformation and orientation of DNA molecules with respect to the direction of Poiseuille flow: v_0, maximum hydrodynamic flow velocity; v_E, velocity due to electrophoresis; θ, attack angle; F_t, tangential drag force; F_n, normal drag force; F_D, net drag force; and F_L, lift force.

The migration of particles relative to a fluid can be considered as being identical to having fluid flow over the particles with the same velocity but opposite in direction. Since the equations

(27) Smith, D. E.; Chu, S. *Science* **1998**, *281*, 1335−1340.
(28) Smith, D. E.; Habcock, H. P.; Chu, S. *Science* **1999**, *283*, 724−727.
(29) Shrewsbury, P. J.; Muller, S. I.; Liepmann, D. *Biomed. Microdevices* **2001**, *3*, 225−238.
(30) Li, L.; Larson, G. *Macromolecules* **2000**, *33*, 1411−1415.
(31) Odegaard-Jensen, A.; Elvingson, C.; Hakansson, C. *Macromol. Theory Simul.* **1996**, *5*, 663−672.
(32) Kang, S. H.; Shortreed, M. R.; Yeung, E. S. *Anal. Chem.* **2001**, *73*, 1091−1099.
(33) Tam, C. K. W.; Hyman, W. A. *J. Fluid Mech.* **1973**, *59*, 177−185.

governing pressure and stress of flow on particles are linear, we may consider the flow as the superposition of a flow aligned with the reference axis and a flow normal to the axis. As described above, the angle θ is the direction of electrophoretic motion of DNA molecules with respect to the reference axis of the deformed DNA molecules. Figure 7a corresponds to the results in Figure 4, in which hydrodynamic flow is from cathode (−) to anode (+). The electrophoretic velocity v_E is decomposed into a tangential component, $v_E \cos \theta$ and a normal component $v_E \sin \theta$.[34] To calculate the drag force on the DNA molecules, first we have to introduce another concept: particle Reynolds number, Re_p, which is defined as

$$Re_p = v_E a\rho/\eta \tag{3}$$

where a is the radius of the DNA molecule, ρ is the density of the fluid, and η is the fluid viscosity. v_E is the electrophoretic velocity, which equals the product of the electrophoretic mobility μ and the electric field E. v_E in Figure 4 can be calculated as $v_E = \mu E = 166\ \mu\text{m s}^{-1}$. If $a \sim 1\ \mu$m, we obtain a small Re_p of 1.66×10^{-4}. Therefore, the drag forces associated with the two velocity components can be calculated with the Stokes drag equation,

$$F_t = c_t'\eta v_E \cos \theta \tag{4}$$

$$F_n = c_n'\eta v_E \sin \theta \tag{5}$$

where c_t' and c_n' are tangential and normal drag force coefficients that are dependent on the shape of the DNA molecules. The subscripts t and n denote tangential and normal components. For an ellipsoid with a maximum radius of a and a length of b, c_t' and c_n' can be expressed as[35]

$$c_t' = 6\pi a((4 + e)/5) \tag{6}$$

$$c_n' = 6\pi a((3 + 2e)/5) \tag{7}$$

where e is the eccentric ratio of the ellipsoid defined as $e \equiv b/a$. For needlelike particles ($e \rightarrow \infty$), c_t' and c_n' are described by the following approximate relationships:

$$c_t' = 2\pi b/(\ln 2e - 0.5) \tag{8}$$

$$c_n' = 4\pi b/(\ln 2e + 0.5) \tag{9}$$

In Figure 7, we use an ellipsoid to represent the shape of a DNA molecule for simplicity. The actual shape of DNA molecules may also be spheroidal or needlelike, depending on the shear rate G and the DNA size, and may also fluctuate continuously.[32] F_L, the lift force perpendicular to the flow axis, and F_D, the drag force parallel to the flow axis, are then given by

$$F_L = F_n \cos \theta - F_t \sin \theta = \frac{\eta v_E \sin 2\theta (c_n' - c_t')}{2} \tag{10}$$

$$F_D = F_n \sin \theta + F_t \cos \theta = \eta v_E (c_n' \cos^2 \theta + c_n' \sin^2 \theta) \tag{11}$$

The lift force F_L causes DNA molecules to move in a direction normal to the electrophoretic and Poiseuille flow direction. In the following, we will use eq 10 to interpret the results in Figures 2−5.

(1) In Figure 2, $v_E = 0$. Therefore, if the inertial effect is neglected (due to the low Reynolds number), eq 10 predicts no lift force and, thus, no lateral migration. That is consistent with our results in Figure 2.

(2) In Figure 3, the shear gradient $G = 0$. In this case, DNA molecules are oriented with the flow. That is, the reference axes of the molecules coincide with the flow direction, or $\theta = 0$. From eq 10, we find that $F_L = 0$. Furthermore, if we consider undeformed DNA molecules as spheres under uniform flow or electric field, the eccentric ratio, $e = 1$. So, $c_t' = c_n' = 6\pi a$, and $F_L = 0$. This explains our results in Figure 3.

(3) In Figure 4, DNA molecules are deformed by the shear flow, such that $0 < \theta < \pi/2$ and the eccentric ratio $e > 1$. Comparing eqs 6 and 7, we can see that $c_n' > c_t'$, thus $F_L > 0$ according to eq 10. Therefore, there exists an inward lift force as shown in Figure 7a. Similar results are obtained if we consider DNA molecules as being deformed to a needlelike shape. According to eqs 8 and 9, we also find that $c_n' > c_t'$, and $F_L > 0$.

(4) In Figure 7b, the direction of v_E is opposite to that in Figure 7a. This can be described by either adding a negative sign to v_E on the right-hand side of eq 10 or by substituting θ with $\pi - \theta$. Both give a negative lift force, which means the force and in turn radial migration is toward the wall of the capillary. This corresponds to the results in Figure 5.

The axial migration velocity was found to be dependent on the electric field, hydrodynamic flow velocity, and ionic strength (data not shown). Higher electric field, higher hydrodynamic flow velocity, and lower ionic strength gave faster lateral migration. Higher hydrodynamic flow velocity also resulted in a narrower DNA zone around the axis when the flow was from cathode to anode. This can be attributed to the large shear gradient away from the center region. Molecules outside that region will be highly deformed and will be quickly focused to the center. The lateral migration was also found to be size dependent. Larger molecules moved faster and clustered closer to the axis while smaller molecules moved slower and their focused position spans a larger region around the axis.

APPLICATION

In CE, hydrodynamic flow due to differential pressure at the two ends of the capillary is generally avoided in order to reduce band broadening. However, in the absence of gravity-induced hydrodynamic flow, there can still be Poiseuille flow if the electroosmotic driving force in not uniform along the capillary column. A common occurrence is that the injected sample zone has a different ionic strength, pH, or viscosity compared to that of the running buffer. In microfluidic devices, different electric field strengths in the different channels also lead to the same effect. To illustrate axial migration under such a condition, we filled the entire column of a fresh capillary that had been rinsed with DI H_2O for 4 h with a DNA sample at low ionic strength (0.4 pM in H_2O). Then, buffer vials containing 20 mM NaCl were

(34) Wu, J.; Manasseh *Int. J. Multiphase Flow* **1998**, *24*, 1343−1358.
(35) Panton, R. L. *Incompressible Flow*, 2nd ed.; John Wiley & Sons: New York, 1996; Chapter 21.

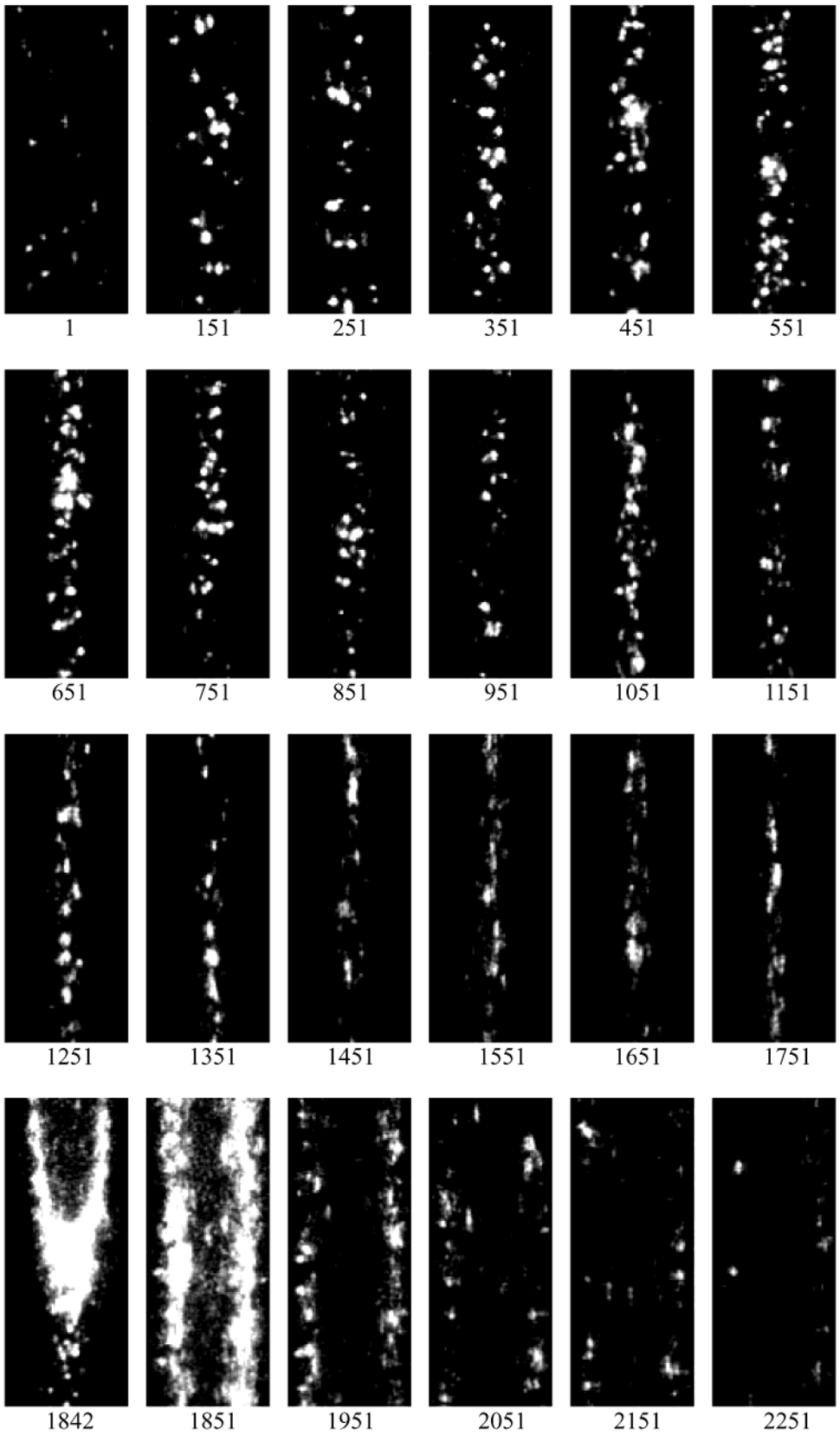

Figure 8. Motion of DNA molecules under nonuniform EOF in a capillary at 10 frames/s: sample, 0.4 pM λ-DNA in water; capillary, 75-μm-i.d. square, 16 cm long with observation at 6 cm from the cathode (bottom) and 10 cm from the anode (top); buffers outside capillary, 20 mM NaCl; electric field, 80 V/cm applied at frame 48; shutter, 20-ms exposure time and 80-ms delay time. All other conditions were the same as in Figure 5.

placed at the two ends of the capillary. Figure 8 shows the sequence of images obtained in this experiment. A complete movie file (movie1.avi) is included as Supporting Information. An electric field of 80 V/cm was applied at frame 48 so that the anode is at

the top and the cathode is at the bottom of the images. To confirm that there were no artifacts, we repeated this experiment by reversing the polarity of the applied voltage. All observations remained identical except that the directions were reversed.

The first 47 frames were monitored without applied electric field. The DNA molecules were stationary except for Brownian motion. This ensured that there was no gravity-induced hydrodynamic flow in the system. Starting in frame 48, DNA molecules moved downward (toward the cathode) as strong EOF (low ionic strength buffer) overcame the electrophoretic motion of the DNA toward the anode. The distribution of molecules across the capillary was initially homogeneous.

On close inspection of the first few hundred frames, it is clear that molecules along the capillary walls moved downward faster than those away from the walls. This difference in velocity is only noticeable for the immediate region near the walls and is not consistent with parabolic flow. We can rule out adsorption or steric effects at the capillary walls, as these effects will slow rather than speed up the molecules. The electroosmotic driving force was restricted to the region close to the walls, but after a short time, the viscous drag of the liquid should have eliminated any sharp velocity gradients. Also, the general theory of EOF predicts a slightly slower, not faster, region at the walls.[17] Indeed, this type of velocity distribution has been reported by us for small particles under electrophoresis even with an axially uniform electroosmotic flow.[36] We attribute this effect to DNA molecules being partially neutralized by the high abundance of positive ions near the capillary surface so that they possess a lower electrophoretic mobility against EOF. The electrostatic influence of the charged surface ranged over several micrometers and was well beyond the thickness of the normal electrical double layer.[37,38]

Starting at frame 150, it is obvious that radial migration of the DNA molecules toward the axis was present. The molecule density near the axis continued to increase while that at the wall decreased. As electrophoresis proceeded, the higher concentration buffer solution entered the capillary (by EOF) to produce a higher ionic strength zone at the anodic end (top). In that zone, the electric field strength as well as the electroosmotic driving force became lower (charge shielding at the wall). The flow profile at the observation region was opposite to that in Figure 7b because bulk flow at the axis was retarded due to the need to pull the slow-moving zone (at the top) into the capillary while maintaining the high electroosmotic driving force at the wall. According to the equations above, DNA molecules will migrate toward the axis rather than away from it.

At still longer times, the DNA molecules gradually slowed until coming to a virtual stop around frame 530. Then the direction of motion reversed (starting around frame 650), i.e., from cathode to anode. This is because the average EOF in the column gradually decreased as the high ionic strength buffer filled a larger and larger fraction of the capillary. At some point, the electrophoretic mobility of the DNA just balanced the opposing (average) EOF to achieve zero axial velocity. Beyond that point, EOF was no longer strong enough to overcome the natural migration of DNA molecules toward the anode.

The movement of DNA molecules toward the anode became faster and faster as electrophoresis progressed, from frame 650 through frame 1800. As the high ionic strength zone moved into the capillary, the zone with the original (low) ionic strength became shorter and shorter. Since the applied voltage was dropped primarily across the low ionic strength zone, the electric field and in turn the DNA velocity in the observation region gradually increased.

Eventually, the high ionic strength zone would go past the detection region. This occurred around frame 1842. The reason DNA molecules were stacked at the zone boundary was because their electrophoretic driving force suddenly decreased on entering the high ionic strength region due to a combination of the lower electric field and decreased ζ potential from charge shielding. The parabolic flow profile of this zone is clearly evident in Figure 8. The direction of the parabola reflects the advancing liquid front at the axis and a slower velocity for the front near the walls.

In the high ionic strength zone, the wall generated a slower EOF such that the bulk liquid was pulled forward faster in the center by the sample zone that passed. This is the exact situation depicted in Figure 7b. Therefore, the DNA molecules were all concentrated at the walls after frame 1842. Close inspection reveals that the DNA molecules were moving away from the anode; i.e., they changed directions at the boundary. This is because strong average EOF (toward the cathode) was still driven by the low ionic strength zone that went past the observation region to overcome the electrophoretic driving force of the DNA (toward the anode).

At very long times (see movie2.avi in Supporting Information), the velocity of the DNA molecules gradually became slower as a result of a decreasing EOF as the low ionic strength zone moved out of the capillary. At around frame 800 of the second movie (280 s after the start of the experiment), the velocity had slowed to a point where reversal of molecular movement was present. This was more pronounced near the walls where the parabolic bulk flow was slower. Eventually, all molecules migrated toward the anode, indicating that EOF was no longer able to overcome the electrophoretic motion of DNA. The velocities became more and more homogeneous across the capillary as the outside buffer gradually filled the entire capillary column; i.e., the traditional flat EOF profile was restored. Without the shear flow gradients, the molecules were also redistributed uniformly across the channel as predicted by eq 10 and Figure 3.

CONCLUSION

We have demonstrated that the radial migration of DNA molecules in capillary electrophoresis with applied Poiseuille flow can be attributed to the deformation and orientation of DNA molecules. By analyzing the forces on the oriented DNA molecules due to electrophoretic migration against shear flow, we derived an expression for the lift force that caused the radial migration. This mechanism explains our results very well and may provide a basis for quantitative study of the factors governing the radial migration. It is possible that these results can be extended to other macromolecules and particles. Fast focusing into the axial region as in Figure 4 may provide an alternative to the sheath flow in flow cytometry. With the addition of electroosmotic flow, molecules can be further driven back or forth (in addition to being focused radially) or kept stationary at a detection window. Radial

(36) Taylor, J. A.; Yeung, E. S. *Anal. Chem.* **1993**, *65*, 2928−2932.
(37) Iki, N.; Kim, Y.; Yeung, E. S. *Anal. Chem.* **1996**, *68*, 4321−4325.
(38) Xu, X.-H.; Yeung, E. S. *Science* **1998**, *281*, 1650−1653.

focusing can also be useful for single-molecule detection, in which every molecule can be concentrated into a small detection volume. By driving molecules away from the wall, the adsorption of analytes can be reduced, which is important in many applications. Size-dependent radial migration may also provide a novel mechanism for size separation of DNA in small channels akin to field-flow fractionation, but with more flexibility because the electric field is applied axially and can be easily reversed. Even in the absence of pressure-induced flow, mismatch in the composition of the sample zone relative to the running buffer in routine CE or differential applied electric fields in microfluidic channels can lead to radial migration of certain analytes.

ACKNOWLEDGMENT

The authors are grateful to James C. Hill and Y. S. Lin for valuable discussions. The Ames Laboratory is operated for the U.S. Department of Energy by Iowa State University under Contract W-7405-Eng-82. This work was supported by the Director of Science, Office of Basic Energy Sciences, Division of Chemical Sciences.

SUPPORTING INFORMATION AVAILABLE

Movie 1: AVI file of frames 1−2000 of Figure 8; 1 s = 10 frames. Movie 2: AVI file of continuation of Figure 8 (frames 2001−4000); 1 s = 10 frames. This material is available free of charge via the Internet at http://pubs.acs.org.

Received for review April 25, 2002. Accepted June 28, 2002.

AC0257344